

## Physical Mapping of BK Virus DNA with *SacI*, *MboII*, and *AluI* Restriction Endonucleases

ROBERT C. A. YANG AND RAY WU\*

*Department of Biochemistry, Molecular and Cell Biology, Cornell University, Ithaca, New York 14853*

Received for publication 16 August 1978

A new restriction endonuclease, *SacI* from *Streptomyces achromogenes* cleaves BK virus (strain MM) DNA into 3 fragments, whereas *MboII* from *Moraxella bovis* and *AluI* from *Arthrobacter luteus* give 22 and 30 fragments, respectively. All these specific DNA fragments were ordered and mapped on the viral genome by two methods: first, by the reciprocal digestion method using uniformly  $^{32}\text{P}$ -labeled DNA; and second, by the partial digestion technique using the single-end  $^{32}\text{P}$ -labeled DNA. This study, together with those reported earlier, defined the location of 90 cleavage sites on the BK virus DNA.

Human papovavirus BKV has been isolated from the urine of immunosuppressed renal allograft recipients (1, 5, 10, 12, 13, 22, 34). A variant of BKV, BKV(MM), was isolated from the urine and the brain tumor of a patient with Wiskott-Aldrich syndrome (31). BKV(MM) is very similar to the prototype BKV, except that the DNA of the former contains three instead of four *HindIII* sites (7).

Serological surveys revealed that about 60 to 80% of human adults have detectable antibodies specific to BKV (3, 4, 15, 27), suggesting that infection with this agent is very common. In addition to its ability to reproduce lytically in human fetal cells, this virus can transform normal hamster cells grown in vitro and, when inoculated into hamsters, induce tumors in vivo (14, 21, 26, 29, 33). Immunological studies have shown that BKV and the well-characterized oncogenic SV40 are closely related but far from being identical (16, 18, 21, 23, 28, 30).

BKV has a circular double-stranded DNA genome with a molecular size similar to that of the SV40 genome (7, 9). DNA-DNA heteroduplex techniques revealed vastly different extents of DNA sequence homology between BKV and SV40, depending on the stringency of the hybridization conditions used (7-9, 11, 19, 20). Under stringent conditions, the heteroduplex (about 11% of the total genome) was formed solely in the late region of the SV40 genome; whereas under less stringent conditions, the heteroduplexes occurred in 92% of the genome (19).

DNA sequence determination will offer the most direct and reliable information for comparing the genomes of BKV and SV40 and for understanding the structure-function relationship of these viruses. With this goal in mind, we made use of a number of restriction endonucle-

ases to specifically cleave BKV DNA into fragments of workable sizes. Once the fragments are physically mapped they will be suitable for extensive DNA sequence analysis. Recently, the sequence of several short BKV DNA fragments has been determined (2, 38).

In this communication, we describe the physical mapping of BKV(MM) DNA by using restriction enzymes *SacI*, *MboII*, and *AluI*.

### MATERIALS AND METHODS

**Cells and viruses.** Plaque-purified BKV (strain MM) obtained from P. M. Howley and K. K. Take-moto was grown in human embryonic kidney cells as described previously (7). Virus stocks were made by infecting the cells at a multiplicity of 0.001 to 0.01 plaque-forming units per cell.

**Preparation of uniformly and terminally labeled DNA.** Detailed procedures have been described previously (35). Briefly, for preparation of uniformly  $^{32}\text{P}$ -labeled BKV DNA, human embryonic kidney cells were infected with BKV at approximately 0.01 to 0.1 plaque-forming units per cell and incubated with carrier-free  $^{32}\text{P}_i$ . After Hirt extraction (6), the viral DNA was purified by equilibrium centrifugation in cesium chloride-ethidium bromide. For preparation of terminally  $^{32}\text{P}$ -labeled DNA, unlabeled restricted BKV DNA fragments were 5'-terminally labeled with [ $\gamma$ - $^{32}\text{P}$ ]ATP and T4 polynucleotide kinase. After purification by polyacrylamide gel electrophoresis, a 5'-terminally labeled fragment was digested with a second restriction enzyme to give two single-end  $^{32}\text{P}$ -labeled fragments.

**Restriction endonuclease cleavage of viral DNA.** Restriction endonucleases *MboII*, *AluI*, *EcoRI*, *HindIII*, *HaeIII*, *HhaI*, *BamHI*, *XbaI*, *KpnI*, *HpaII*, and *PstI* were obtained from New England BioLabs (Beverly, Mass.). *SstI* was purchased from Bethesda Research Laboratories (Rockville, Md.). *MboI* and *SacI* were kindly provided by R. Roberts and J. Szostak, respectively.

The standard cofactor mixture for most of these

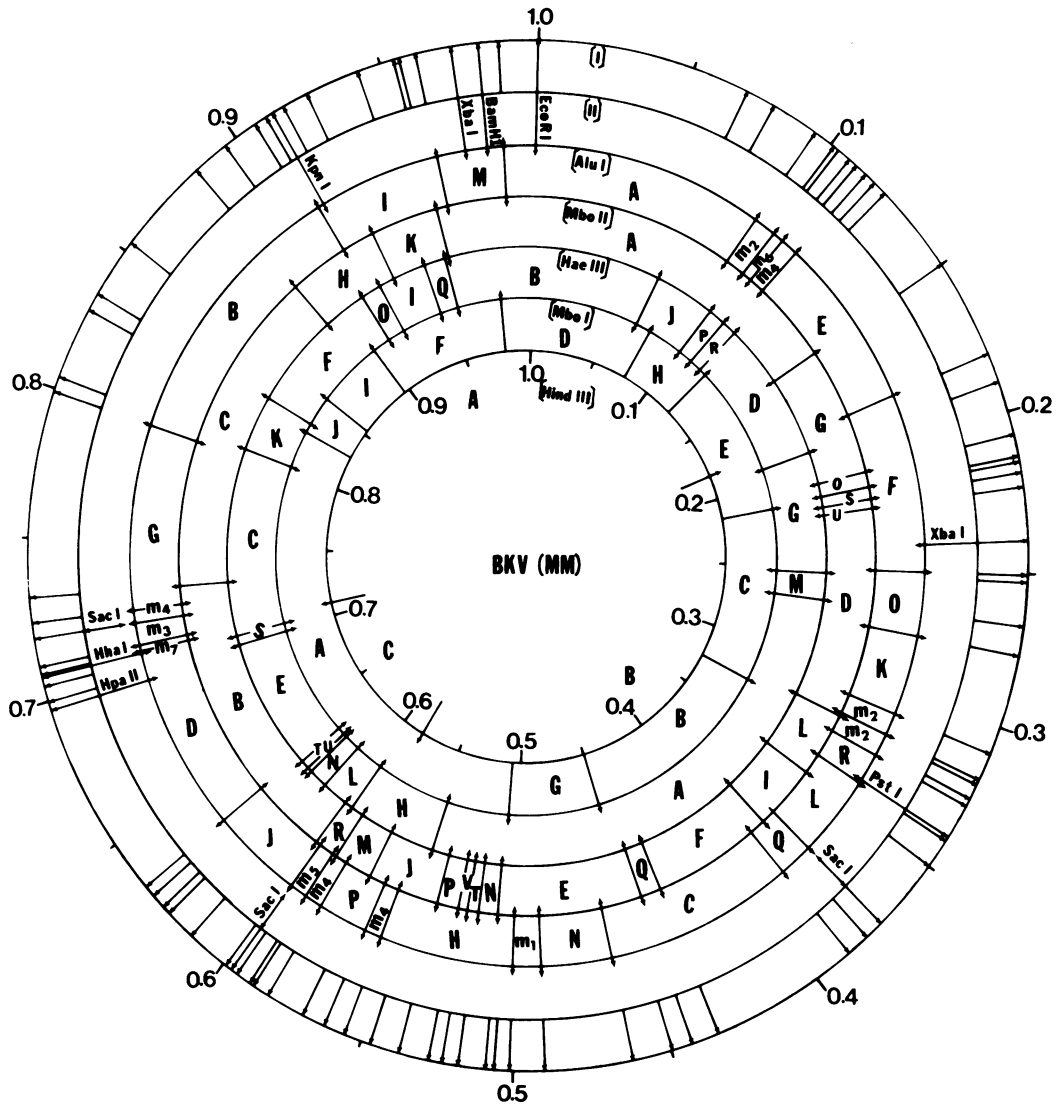


FIG. 1. Detailed physical maps of the BKV genome. The circular double-stranded DNA genome of BKV(MM) is shown with the unique EcoRI site taken as 0 or 1.0 site. The cleavage map of each restriction endonuclease (e.g., AluI), which produces a large number of fragments on the viral DNA, is drawn separately. Circle II includes the cleavage sites of the single-cut enzymes and those of XbaI and SacI. Circle I is the multiple cleavage map consisting of 90 sites derived from the 13 enzymes used. The 3 sites of SacI, 30 sites of AluI, and 22 sites of MboII are mapped as described in this paper. The cleavage sites of HaeIII and MboI were mapped by Yang and Wu (39); those of HindIII, EcoRI, and HpaII were determined by Howley et al. (7); and those of BamHI, KpnI, HhaI, PstI, and XbaI were located by Yang and Wu (38). Map orientation is guided by a key fragment (or site) for each map: HindIII-A (map positions 0.715 to 0.180), MboI-D (0.980 to 0.075), XbaI-B (0.973 to 0.240), SacI-A (0.720 to 0.375), HaeIII-B (0.952 to 0.070), MboII-A (0.954 to 0.149), AluI-A (0.990 to 0.095), BamHI site (0.980), KpnI site (0.915), HhaI site (0.710), HpaII site (0.695), and PstI site (0.340).

restriction enzymes contained 10 mM Tris-hydrochloride (pH 7.5), 7 mM 2-mercaptoethanol, and 7 mM MgCl<sub>2</sub> (36). The cofactor mixture for SacI and SstI contained 80 mM NaCl in addition. For complete digestion, 0.3 U of enzyme per  $\mu$ g of DNA was used. Incubation took place at 37°C for 3 to 15 h. For partial

digestion, single-end <sup>32</sup>P-labeled DNA and smaller amounts of enzyme were used. Samples were taken at 2, 5, 10, 20, and 40 min of incubation time and pooled before electrophoresis.

**Gel electrophoresis and autoradiography.** For monitoring completeness of digestion of unlabeled

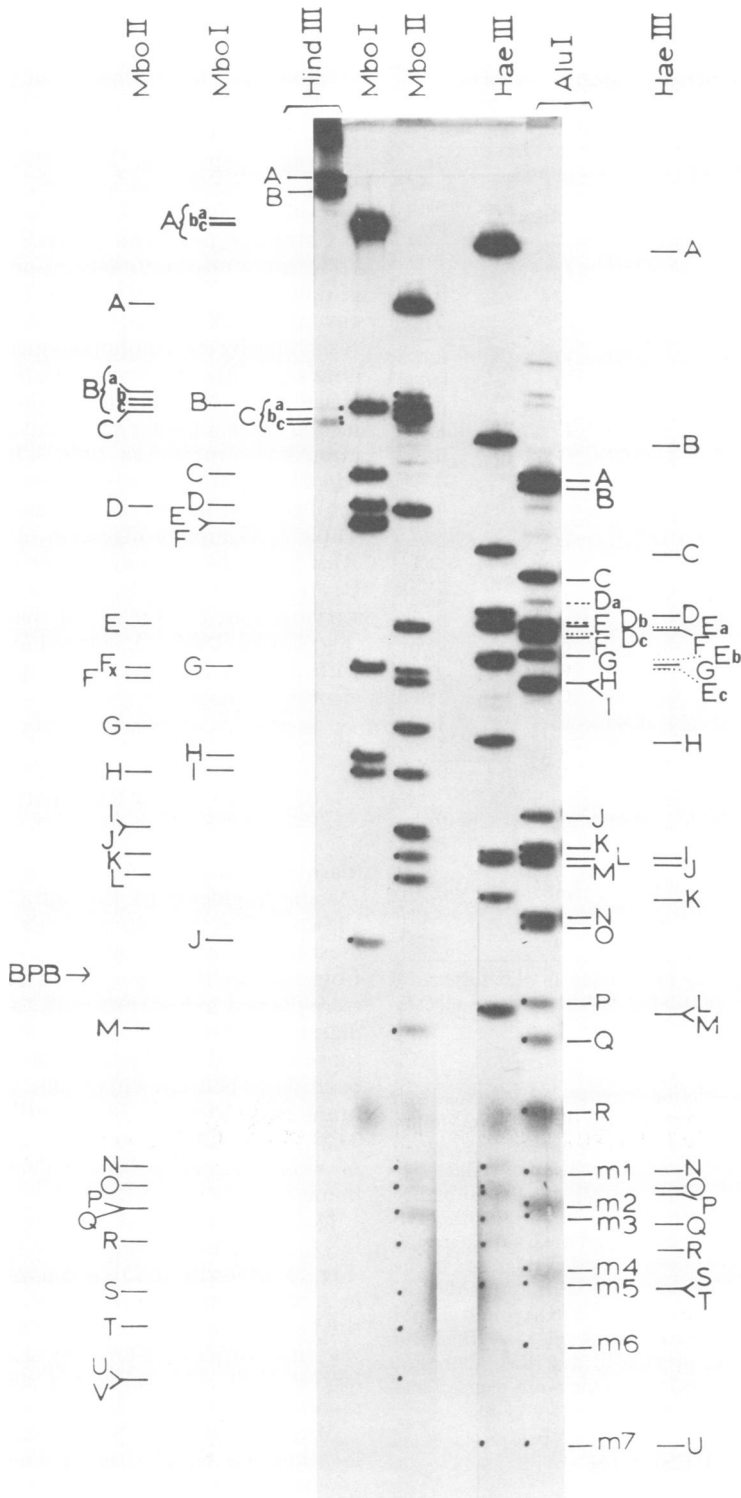


FIG. 2. Electrophoretic patterns of restriction fragments produced by complete digestion of BKV DNA with individual restriction endonucleases. Uniformly  $^{32}\text{P}$ -labeled BKV DNA ( $0.1 \mu\text{g}$ ,  $1.5 \times 10^6 \text{ cpm}/\mu\text{g}$ ) was digested with each restriction endonuclease to completion and fractionated by electrophoresis on a 3.5% polyacrylamide gel. The restriction patterns are indicated and schematically depicted alongside the gel. Size estimation of restriction fragments was carried out according to the published procedures (36). The data are documented in Table 1. BPB, Bromophenol blue dye marker.

TABLE 1. Restriction fragments obtained by complete digestion of uniformly  $^{32}\text{P}$ -labeled BKV(MM) DNA with *SacI*, *MboII*, or *AluI*<sup>a</sup>

<i>SacI</i> fragment	Genome length (%)	<i>MboII</i> fragment	Genome length (%)	<i>AluI</i> fragment	Genome length (%)
A	65.30	A	19.00	A	11.00
B	22.50	B <sub>a</sub>	14.00	B	10.70
C <sub>a</sub>	12.20	B <sub>b</sub>	13.60	C	7.90
C <sub>b</sub>	11.80	B <sub>c</sub>	13.50	D <sub>a</sub>	7.20
C <sub>c</sub>	11.70	C	13.50	D <sub>b</sub>	6.75
		D	9.90	D <sub>c</sub>	6.60
		E	6.80	E	6.40
		F	5.70	F	6.40
		G	5.00	G	6.10
		H	4.30	H	5.50
		I	3.60	I	5.50
		J	3.60	J	3.70
		K	3.35	K	3.45
		L	3.15	L	3.35
		M	1.90	M	3.35
		N	1.15	N	2.75
		O	1.07	O	2.70
		P	0.95	P	2.05
		Q	0.95	Q	1.80
		R	0.80	R	1.40
		S	0.59	m1	1.10
		T	0.50	m2(triplet)	0.94
		U	0.44	m3	0.88
		V	0.44	m4(quartet)	0.65
				m5	0.58
				m6	0.43
				m7	0.20

<sup>a</sup> Genome length as percentage of the total viral DNA molecule is calculated on the basis of electrophoretic mobility.

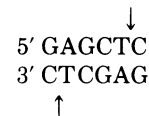
BKV DNA with restriction enzymes, a 1% agarose slab gel of 0.3 by 20 cm containing 0.5  $\mu\text{g}$  of ethidium bromide per ml was used. Electrophoresis was carried out at 75 mA for 4 h. For fractionation of radioactive DNA digests, a slab gel (0.15 by 34 by 40 cm) of 3 to 6% polyacrylamide (ratio of acrylamide to bis-acrylamide, 20:1) was used for electrophoresis at 120 to 150 V until bromophenol blue dye marker migrated to the desired positions. The buffer contained 40 mM Tris-hydrochloride (pH 7.9), 20 mM NaOAc, and 2 mM EDTA. Analytical polyacrylamide gels were dried and autoradiographed as previously described (36). For preparative gels, the gel segments were excised and DNA was eluted as previously described (36).

## RESULTS

For physical mapping of BKV DNA using the cleavage sites of restriction endonucleases, we employed two procedures as described earlier (39): first, the method of reciprocal cleavage using uniformly  $^{32}\text{P}$ -labeled DNA prepared in

vivo; second, the technique of partial cleavage using single-end  $^{32}\text{P}$ -labeled DNA prepared in vitro. The completed *HindIII*, *MboI*, and *HaeIII* cleavage maps (Fig. 1) of BKV (strain MM) DNA were used in locating the unknown cleavage sites of *SacI* (or *SstI*), *MboII*, and *AluI*.

**Cleavage patterns of BKV DNA with restriction endonucleases.** Complete cleavage of uniformly  $^{32}\text{P}$ -labeled BKV DNA with *MboII* gave rise to 22 specific fragments (A through V), resolvable by electrophoresis in a 3.5% polyacrylamide gel (Fig. 2). Size estimation of fragments based on electrophoretic mobility, using the molecular markers, was carried out according to the published procedures (36). The sizes of the *MboII* fragments ranging from 19 to 0.44% of total genome length of BKV are documented in Table 1. Complete digestion of BKV DNA by *AluI* generated 18 major fragments (A through R) and twelve minor fragments (m1 through m7) varying from 11 to 0.20% of the genome length (Fig. 2 and Table 1). Digestion of BKV DNA with *SacI* or *SstI*, which recognizes a hexanucleotide sequence of



(data will be published elsewhere), gave three specific fragments (A through C) (Table 1). As shown in Fig. 2, three particular fragments (indicated as dotted bands a, b, and c), differing from one another by about 5 to 26 base pairs, were present in less than molar amounts in each digest. The presence of two viable deletion mutants other than the original MM strain has been described elsewhere (39). Since both mutants have lost the *HpaII* site (map position 0.69), the small deletion must be located at approximately map position 0.69 on the viral genome.

Double digestion of uniformly labeled BKV DNA, using two restriction enzymes at a time (Fig. 3), gave rise to DNA fragments designated in Arabic numerals prefixed with the names of the two enzymes used (e.g., *MboI-MboII* 1, 2, 3 . . . , in an order of decreasing size where 1 is the largest [36]). The estimated sizes of the fragments are listed in Tables 2 and 3.

**Mapping of the *SacI* cleavage sites.** In locating the three sites of *SacI* on the viral genome, each *SacI* fragment of uniformly  $^{32}\text{P}$ -labeled BKV DNA was isolated and digested with *HindIII* (Fig. 4). Then, each *HindIII* fragment was digested with *SacI* (the gel patterns are not shown). The cleavage patterns were subjected to overlap analysis with respect to the

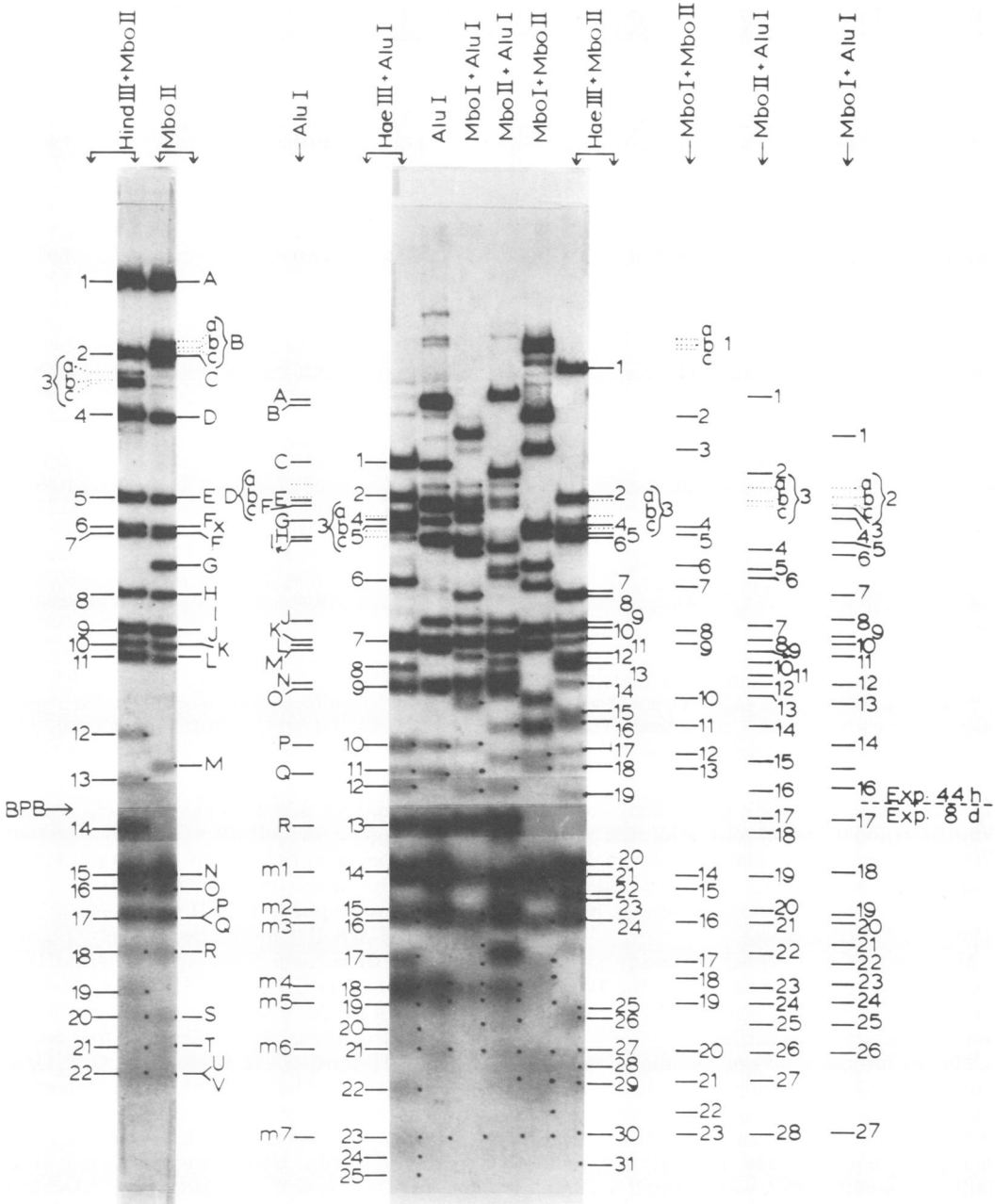


FIG. 3. Electrophoretic patterns of restriction fragments produced by complete digestion of BKV DNA with a combination of two restriction endonucleases. The uniformly labeled DNA (0.2 µg) was digested simultaneously with two enzymes as described in the legend to Fig. 2.

known order of the *Hind*III fragments (7). Upon digestion with *Hind*III, *Sac*I-A gave rise to two subfragments, *Hind*III-*Sac*I 1 and 3; *Sac*I-B gave 2 and 5; and *Sac*I-C gave 4 and 6 (Fig. 4 and Table 4). Reciprocal cleavage of the individual *Hind*III fragments with *Sac*I was similarly

performed. The data are summarized in Table 4. Mapping of the three *Sac*I fragments of the BKV DNA is illustrated as follows: since subfragment *Hind*III-*Sac*I 1 overlaps with *Hind*III-A and *Hind*III-*Sac*I 3 with *Hind*III-B, *Sac*I-A is thus located between *Hind*III-A and

TABLE 2. Restriction fragments obtained by complete digestion of uniformly <sup>32</sup>P-labeled BKV(MM) DNA with a combination of two restriction enzymes as indicated<sup>a</sup>

<i>Hind</i> III- <i>Sac</i> I fragment	Genome length (%)	<i>Xba</i> I- <i>Mbo</i> II fragment	Genome length (%)	<i>Hind</i> III- <i>Mbo</i> II fragment	Genome length (%)	<i>Mbo</i> I- <i>Mbo</i> II fragment	Genome length (%)
1	46.50	1	18.20	1	19.00	1 <sup>b</sup>	14.40
2	21.80	2 <sup>b</sup>	14.00	2	13.50	2	10.00
3	18.70	3	13.50	3 <sup>b</sup>	12.30	3	8.60
4 <sup>b</sup>	11.00	4	7.50	4	9.90	4 <sup>c</sup>	5.90
5	1.23	5	6.80	5	6.80	5	5.70
6	0.98	6 <sup>c</sup>	5.90	6 <sup>c</sup>	5.90	6	4.90
		7	5.70	7	5.70	7	4.50
		8	5.00	8	5.00	8	3.60
		9	4.30	9	4.30	9	3.30
		10	3.60	10	3.60	10	2.50
		11	3.35	11	3.15	11	2.25
		12	3.15	12	2.20	12	1.95
		13	2.22	13	1.75	13	1.85
		14	1.90	14	1.42	14	1.10
		15	1.15	15	1.15	15	1.03
		16	1.07	16	1.07	16	0.88
		17	0.95	17	0.95	17	0.72
		18	0.80	18	0.80	18	0.68
		19	0.59	19	0.66	19	0.58
		20	0.50	20	0.59	20	0.43
		21	0.44	21	0.50	21	0.35
				22	0.44	22	0.26
						23	0.20

<sup>a</sup> Genome length is estimated as in Table 1.

<sup>b</sup> Three species of DNA (a, b, c) were observed in this fragment. The differences in length between a and b and b and c are 0.4 and 0.1%, respectively. For example, *Hind*III-*Sac*I 4<sub>a</sub> (11.00%), 4<sub>b</sub> (10.60%), and 4<sub>c</sub> (10.50%).

<sup>c</sup> This fragment corresponds to *Mbo*II-Fx, an incomplete product corresponding to *Mbo*II-F plus Q (see text).

-B. Similarly, *Sac*I-B is located between *Hind*III-B and -C, and *Sac*I-C is located between *Hind*III-C and -A. The derived order of the *Sac*I fragments is as shown on circle II of Fig. 1. The *Sac*I map is oriented by *Sac*I-A at map positions 0.720 to 0.375 (clockwise).

**Mapping of the *Mbo*II cleavage sites.** In locating the 22 sites of *Mbo*II on the BKV genome, two techniques were used for obtaining complementary information.

The reciprocal cleavage technique was first applied using the known positions of the *Hind*III, *Xba*I, *Mbo*I, and *Hae*III cleavage sites as the physical markers on BKV DNA. As shown in Fig. 5a, each isolated *Hind*III fragment of uniformly labeled DNA was digested to completion with *Mbo*II. *Hind*III-A, upon cleavage with *Mbo*II, gave *Hind*III-*Mbo*II 1, 2, 8, 10, 11, and 12. Similarly, *Hind*III-B gave 4, 5, 6, 7, 9 (doublet), 11, 13, 14, 15, 16, 17 (doublet), 20, 21, and 22 (doublet); *Hind*III-C gave 3, 18, and 19. The results are summarized in Table 5. Apparently, *Mbo*II-B, -G, and -M were the only fragments cleaved by *Hind*III. Reciprocal digestion of *Mbo*II-B, -G, and -M separately with *Hind*III gave rise to the cleavage patterns shown in Fig. 5a. *Mbo*II-B gave two subfragments, *Hind*III-

*Mbo*II 3 and 12; *Mbo*II-G gave 11 and 13; and *Mbo*II-M gave 14 and 19 (Table 5). Overlap analysis was then carried out to determine the order of the *Mbo*II fragments on the genome. *Mbo*II-B overlapped *Hind*III-C and *Hind*III-A by *Hind*III-*Mbo*II 3 and 12, respectively (Fig. 6). Thus, *Mbo*II-B spans from a part of *Hind*III-C to a part of *Hind*III-A. *Mbo*II-G and -M were located in a similar manner. A preliminary order of *Mbo*II fragments was obtained as follows: (i) -B-(A, C, H, K)-G-(D, E, F, I, J, L, N, O, P, Q, S, T, U, V)-M-R-. The order of the fragments in parentheses was undetermined.

Next, each uniformly labeled *Xba*I fragment was digested with *Mbo*II into completion (Fig. 5B). In a reciprocal digestion, the individual *Mbo*II fragments were digested with *Xba*I (gel patterns not shown). The results are documented in Table 5. After overlap analysis, a partial *Mbo*II fragment order was obtained: (ii) -A-(G, O, S, U)-D-(B, C, E, F, H, I, J, K, L, M, N, P, Q, R, T, V)-, where fragment A was located at map positions 0.954 to 0.149 (see also Fig. 1). In order (i), the map positions of *Mbo*II-G were at 0.149 to 0.199. Therefore, *Mbo*II-G is located next to -A.

Reciprocal cleavage (gel not shown) of indi-

TABLE 3. Restriction fragments obtained by complete digestion of uniformly <sup>32</sup>P-labeled BKV(MM) DNA with a combination of two restriction enzymes as indicated<sup>a</sup>

<i>Hae</i> III- <i>Mbo</i> II fragment	Genome length (%)	<i>Mbo</i> I- <i>Alu</i> I fragment	Genome length (%)	<i>Mbo</i> II- <i>Alu</i> I fragment	Genome length (%)	<i>Hae</i> III- <i>Alu</i> I fragment	Genome length (%)
1	12.60	1	9.20	1	11.00	1	7.90
2	6.80	2 <sup>b</sup>	7.20	2	7.60	2	6.75
3 <sup>b</sup>	6.10	3	6.40	3 <sup>b</sup>	7.20	3 <sup>b</sup>	6.20
4 <sup>c</sup>	5.90	4	6.10	4	5.30	4	6.20
5	5.60	5	5.50	5 <sup>d</sup>	4.90	5	5.95
6	5.50	6	5.20	6	4.65	6	4.55
7	4.25	7	4.20	7	3.70	7	3.35
8	4.20	8	3.70	8	3.45	8	3.00
9	3.70	9	3.45	9	3.35	9	2.70
10	3.60	10	3.35	10	3.10	10	2.05
11	3.40	11	3.20	11	2.85	11	1.80
12	3.20	12	2.75	12	2.75	12	1.65
13	3.05	13	2.55	13	2.60	13	1.40
14	2.76	14	2.05	14	2.25	14	1.10
15	2.40	15	1.80	15	1.95	15	0.94
16	2.30	16	1.65	16	1.62	16	0.88
17	2.00	17	1.40	17	1.45	17	0.75
18	1.85	18	1.10	18	1.35	18	0.65
19	1.60	19	0.92	19	1.10	19	0.58
20	1.15	20	0.88	20	0.94	20	0.50
21	1.10	21	0.79	21	0.88	21	0.43
22	1.00	22	0.72	22	0.75	22	0.32
23	0.97	23	0.65	23	0.65	23	0.20
24	0.89	24	0.58	24	0.58	24	0.15
25	0.78	25	0.50	25	0.50	25	0.10
26	0.54	26	0.43	26	0.43		
27	0.53	27	0.20	27	0.35		
28	0.43			28	0.20		
29	0.38						
30	0.33						
31	0.20						

<sup>a</sup> Genome length is estimated as in Table 1.<sup>b</sup> See Table 2, footnote b.<sup>c</sup> See Table 2, footnote c.<sup>d</sup> An incomplete product corresponding to *Mbo*II-*Alu*I 6 plus 21 (see text).TABLE 4. Analysis of uniformly <sup>32</sup>P-labeled individual *Hind*III fragments and *Sac*I fragments after reciprocal digestion with *Sac*I and *Hind*III respectively

<i>Hind</i> III fragment	Release of <i>Hind</i> III- <i>Sac</i> I subfragment	<i>Sac</i> I cleavage site/ <i>Hind</i> III fragment	<i>Sac</i> I fragment	Release of <i>Hind</i> III- <i>Sac</i> I subfragment	<i>Hind</i> III cleavage site/ <i>Sac</i> I fragment
A	1, 6	1	A	1, 3	1
B	2, 3	1	B	2, 5	1
C <sup>a</sup>	4, <sup>a</sup> 5	1	C <sup>a</sup>	4, <sup>a</sup> 6	1

<sup>a</sup> See Table 2, footnote b.

vidual *Mbo*I fragments with *Mbo*II and vice versa resulted in the ordering of *Mbo*II fragments as follows: (iii) -A-(G, O)-S-(D, U)-L-(F, I, Q)-E-(B, J, M, N, P, R, T, V)-C-H-K- (Fig. 7a). In a similar way, another order (Fig. 7b)

derived through *Hae*III-*Mbo*II reciprocal cleavage (gel patterns not shown) is shown below: (iv) -K-A-G-(O, S, U)-D-(E, F, I, L, N, P, Q, T, V)-J-M-R-B-C-H-. The results obtained from these four sets of reciprocal cleavage (i to iv) are complementary. This enables us to deduce the following order of *Mbo*II fragments: (v) -A-G-O-S-U-D-L-(F, I, Q)-E-(N, P, T, V)-J-M-R-B-C-H-K-.

The two uncertain regions (in parentheses) of the order of the *Mbo*II fragments were then solved by the partial digestion technique. Several single-end <sup>32</sup>P-labeled DNA fragments used for partial cleavage with *Mbo*II are listed in Table 6, together with the result of the order of component *Mbo*II fragments. Two typical gel patterns are shown in Fig. 8. Partial digestion of single-end labeled (<sup>32</sup>P at the *Hind*III site) *Xba*I-A *Hind*III-B (map positions 0.24 to 0.58 on Fig. 1) gave rise to 12 radioactive bands (Fig. 8a)

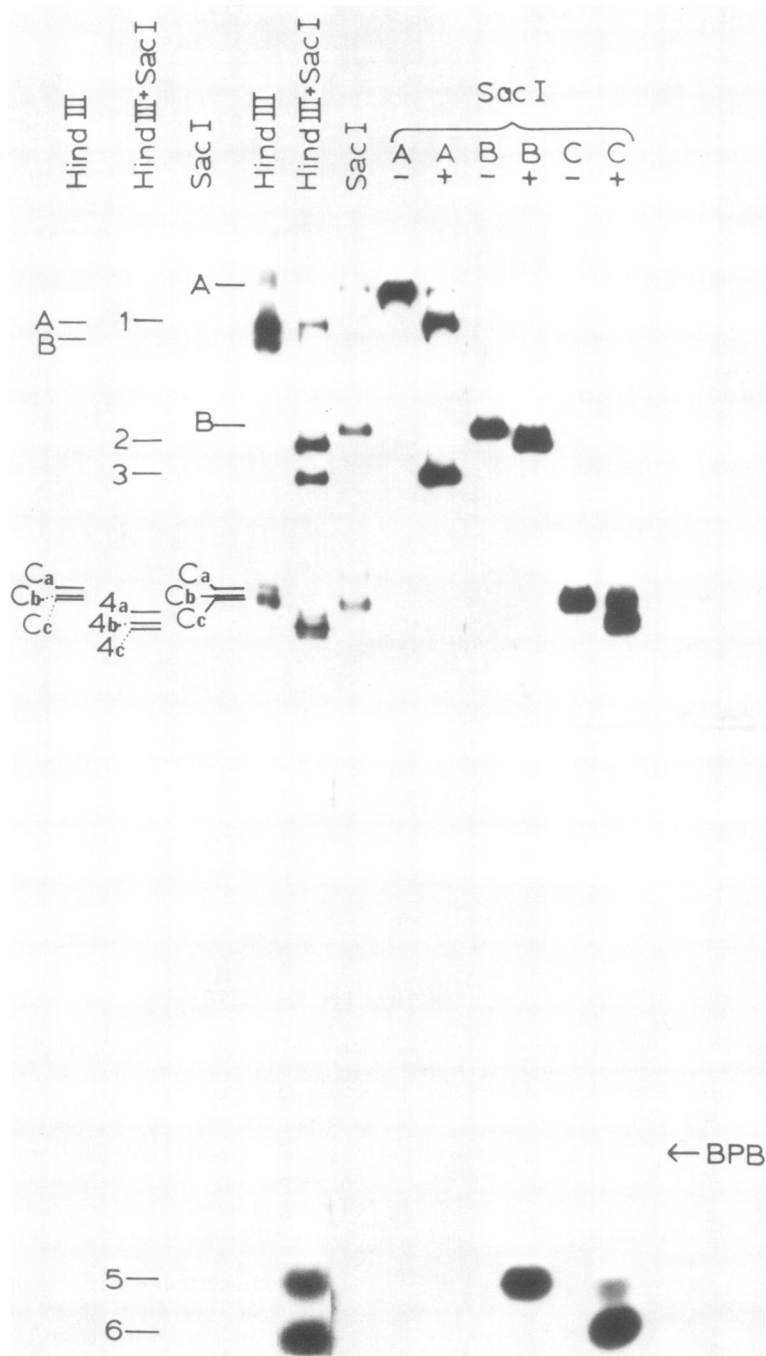


FIG. 4. Cleavage patterns of individual SacI fragments with HindIII. Each isolated SacI fragment ( $0.5 \times 10^3$  to  $1.5 \times 10^3$  cpm) derived from uniformly labeled BKV DNA was incubated with an excess amount of HindIII. Each digest was indicated on top as A+, B+, and C+, whereas A-, B-, and C- were the untreated SacI fragments run alongside as references. Apparently, the digestion was not complete. Some weak bands of undigested SacI-A, -B, and -C were still seen in the + lanes. But the patterns are clear. Three marker digests, SacI, HindIII+ SacI, and HindIII, were run in the same gel.



TABLE 5. Analysis of uniformly <sup>32</sup>P-labeled individual restriction fragments after reciprocal digestion with a second restriction endonuclease

<i>Hind</i> III frag- ment	Release of <i>Hind</i> III- <i>Mbo</i> II subfrag- ment	<i>Mbo</i> II cleav- age site/ <i>Hind</i> III frag- ment	<i>Mbo</i> II frag- ment <sup>a</sup>	Release of <i>Hind</i> III- <i>Mbo</i> II subfrag- ment	<i>Hind</i> III cleav- age site/ <i>Mbo</i> II frag- ment	<i>Xba</i> I frag- ment	Release of <i>Xba</i> I- <i>Mbo</i> II subfrag- ment	<i>Mbo</i> II cleav- age site/ <i>Xba</i> I frag- ment	<i>Mbo</i> II frag- ment <sup>a</sup>	Release of <i>Xba</i> I- <i>Mbo</i> II subfrag- ment	<i>Xba</i> I cleav- age site/ <i>Mbo</i> II frag- ment
A	1, 2, 8, 10, 11, 12	5	B <sup>b</sup> G	3, <sup>b</sup> 12 11, 13	1 1	A <sup>b</sup>	2, <sup>b</sup> 3, 4 5, 6, <sup>c</sup> 7, 9, 10, 10, 11, 12, 14, 14, 15, 17, 17, 18, 20, 21	18	A	1, 14	1
B	4, 5, 6, <sup>c</sup> 7, 9, 9, 11, 13, 14, 15, 16, 17, 17, 20, 21, 22, 22	16	M	14, 19	1	B	1, 8, 13, 16, 19, 21	5	D	4, 13	1
C <sup>b</sup>	3, <sup>b</sup> 18, 19	2									

<sup>a</sup> The rest of the fragments which received no cleavage from the second enzyme are not listed.

<sup>b</sup> See Table 2, footnote *b*.

<sup>c</sup> This fragment corresponds to *Mbo*II-Fx (see text).

corresponding to the 12 partially cleaved products that share the common <sup>32</sup>P-labeled end. These bands were subjected to size estimation for the *Mbo*II fragments. The derived order of the *Mbo*II fragments for each radioactive band is indicated alongside the gel pattern. Figure 8b shows the partial digestion with *Mbo*II of single-end labeled (<sup>32</sup>P at the *Mbo*I site) *Hind*III-B *Mbo*I-A (0.51 to 0.58 on Fig. 1). The derived orders obtained from the two aforementioned samples are complementary. Thus the fragment order of *Mbo*II shown (v) is completed as follows: -A-G-O-S-U-D-L-I-F-Q-E-N-T-V-P-J-M-R-B-C-H-K-. The results obtained from other sets of partial cleavages have totally confirmed this order (Table 6) as well as the partial order derived from experiments i to iv.

**Mapping of the *Alu*I cleavage sites.** In locating the 30 sites of *Alu*I on the BKV genome, similar procedures were applied. Each uniformly <sup>32</sup>P-labeled *Alu*I fragment was cleaved separately with each of the following enzymes: *Hind*III, *Mbo*I, *Mbo*II, and *Hae*III; and vice

versa, each *Hind*III, *Mbo*I, *Mbo*II, and *Hae*III fragment was cleaved with *Alu*I. The resulting cleavage products (Tables 2 and 3) were subjected to overlap analysis for ordering the *Alu*I fragments on the genome. In Fig. 9 are shown two typical examples of reciprocal cleavage (gel patterns are not shown). The two preliminary orders of *Alu*I fragments derived from *Mbo*I-*Alu*I (Fig. 9a) as well as *Hae*III-*Alu*I (Fig. 9b) reciprocal cleavages are complementary to each other. Thus, the fragment order can be deduced as follows: -I-M-A-m2-m6-m4-E-F-O-(K, m2)-m2-(L, Q, R)-C-(N, m1)-H-(P, m4, m4)-m5-J-D-(G, m3, m4, m7)-B-. Similarly, the results obtained by *Mbo*II-*Alu*I reciprocal cleavage (data not shown), provided the following order, -m4-P-m4- (see the italicized section of the order just shown). The order of *Alu*I fragments is refined as: -I-M-A-m2-m6-m4-E-F-O-(K, m2)-m2-(L, Q, R)-C-(N, m1)-H-m4-P-m4-m5-J-D-(G, m3, m4, m7)-B-.

Information obtained by partial cleavages of several single-end labeled DNA fragments with

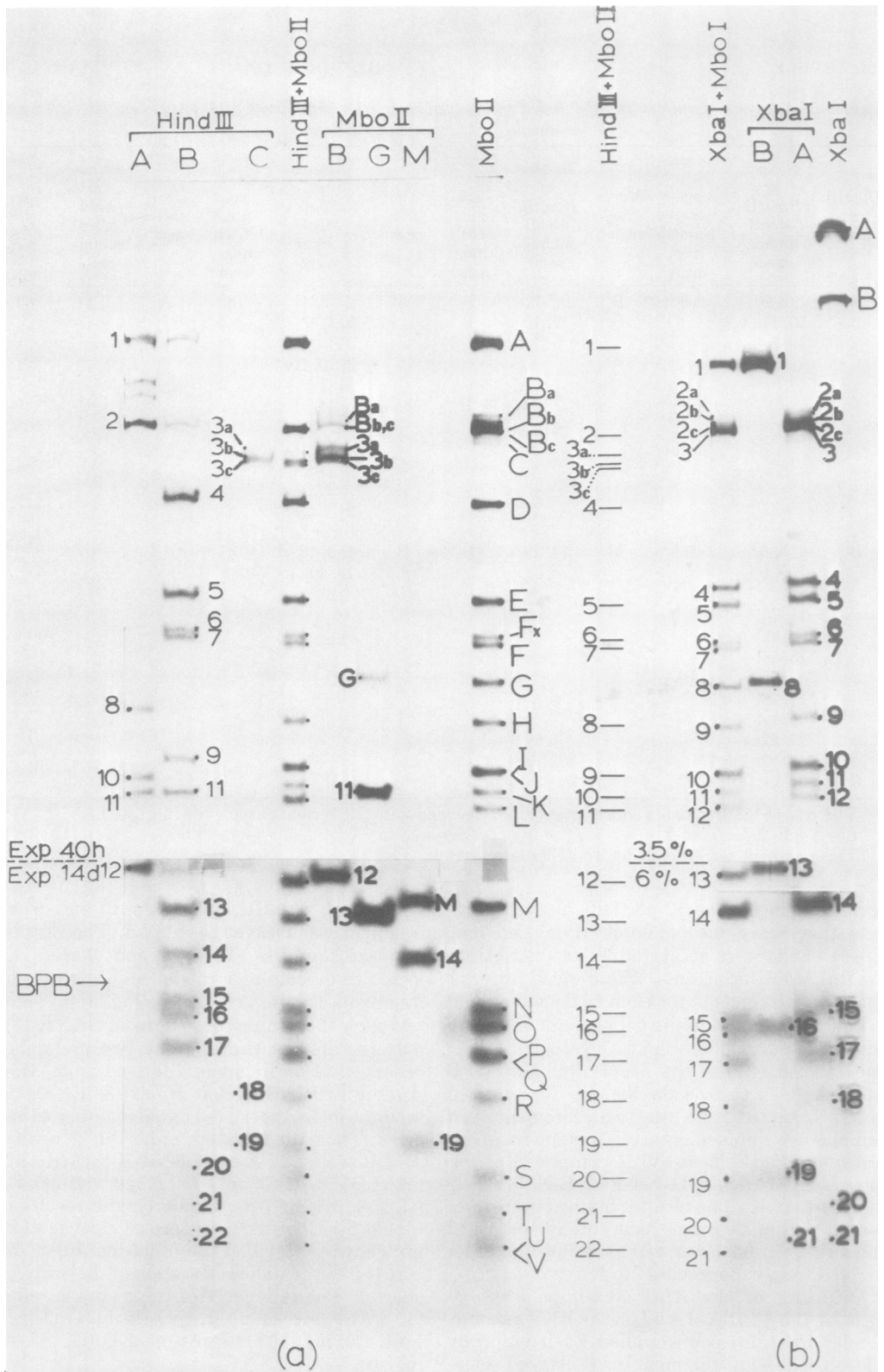


**FIG. 5. (a) Gel patterns of BKV HindIII-MboII reciprocal cleavage products. Each isolated uniformly  $^{32}\text{P}$ -labeled HindIII fragment was digested with MboII to completion, and vice versa each MboII fragment which contains HindIII site was digested with HindIII. The digests, as indicated on top of the gel, were fractionated in the same gel. The BKV DNA digests, HindIII+ MboII and MboII, were run together as markers. (b) Cleavage of individual XbaI fragments with MboII. Individual radioactive XbaI fragments were isolated and then digested with MboII. The electrophoretic gel patterns were analyzed.**

*AluI* (Table 7) has completed the order of *AluI* fragments as follows: -I-M-A-m2-m6-m4-E-F-O-K-m2-m2-R-L-Q-C-N-m1-H-m4-P-m4-m5-J-D-m7-m3-m4-G-B- (Fig. 1).

**DISCUSSION**

Detailed physical mapping of a defined DNA molecule by use of restriction endonucleases has great potential value on studies in the structure-



FIG. 6. Overlap analysis for ordering an *MboII* restriction fragment. The known positions of two *HindIII* fragments are drawn as indicated. The position of an *MboII* fragment is to be determined (shown above the linear map). *MboII-B*, upon cleavage with *HindIII*, released *HindIII-MboII* 3 and 12 which are also subfragments of *HindIII-C* and *A* (See Fig. 5a and Table 5), respectively. Thus, *MboII-B* overlaps *Hind-C* and *A* by *HindIII-MboII* 3 and 12, respectively.

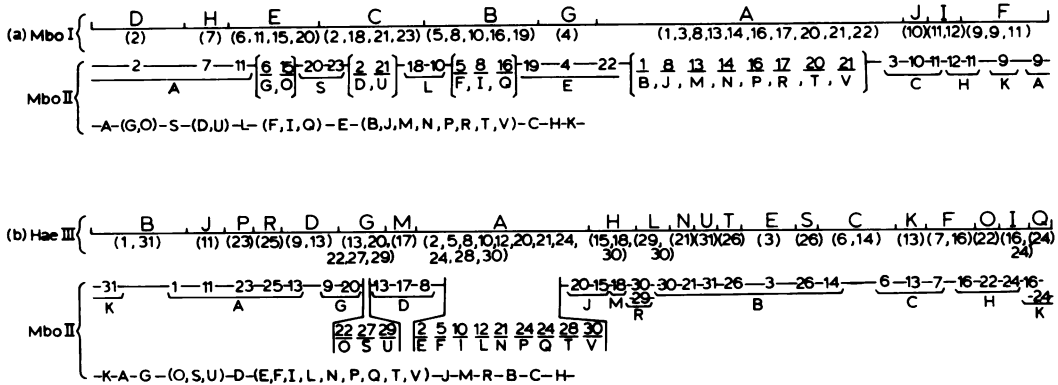


FIG. 7. (a) Overlap analysis on the *MboI-MboII* reciprocal cleavage patterns. The circular genome of BKV is represented in the linear form. The specific order of the *MboI* fragments is shown on line *MboI*. The component *MboI-MboII* subfragments belonging to each *MboI* fragment are also included. In lines *MboII*, each *MboII* fragment is specifically located according to the overlapping of its component *MboI-MboII* subfragments with those of the *MboII* fragments. The resulting order of the *MboII* fragments is summarized. (b) Overlap analysis on the *HaeIII-MboII* reciprocal cleavage patterns. The gel patterns of the *HaeIII-MboII* reciprocal cleavage are not shown. Explanation of lines -*HaeIII* and -*MboII* is similar to that of (a).

TABLE 6. Single-end <sup>32</sup>P-labeled DNA fragments used for partial cleavage with *MboII* enzyme

DNA fragment <sup>a</sup>	Map position	5'-Labeled site	Derived order of <i>MboII</i> fragments <sup>b</sup>
<i>XbaI-A HindIII-A</i>	0.72-0.97	<i>HindIII</i>	B <sub>2</sub> -C-H-K-A <sub>2</sub>
<i>XbaI-B HindIII-A</i>	0.97-0.18	<i>HindIII</i>	G <sub>1</sub> -A <sub>1</sub>
<i>XbaI-A HindIII-B</i>	0.24-0.58	<i>HindIII</i>	M <sub>1</sub> -J-P-V-T-N-E-Q-F-I-L-D <sub>1</sub>
<i>XbaI-B HindIII-B</i>	0.18-0.24	<i>HindIII</i>	G <sub>2</sub> -O-S-U-D <sub>2</sub>
<i>HhaI-A HindIII-C<sup>c</sup></i>	0.58-0.71	<i>HindIII</i>	M <sub>2</sub> -R-B <sub>1</sub> <sup>c</sup>
<i>PstI-A MboI-B</i>	0.34-0.45	<i>MboI</i>	E <sub>2</sub> -Q-F-I-L <sub>2</sub>
<i>MboI-A HindIII-B</i>	0.51-0.58	<i>HindIII</i>	M <sub>1</sub> -J-P-V-T-N—
<i>HindIII-B MboI-A</i>	0.51-0.58	<i>MboI</i>	E <sub>3</sub> -N-T-V-P-J-M <sub>1</sub>

<sup>a</sup> *XbaI-A* and -B are located at map positions 0.24 to 0.97 (clockwise) and 0.97 to 0.24, respectively.

<sup>b</sup> The left-most fragment bears the <sup>32</sup>P label.

<sup>c</sup> Three fragments of close sizes were observed as noted in Table 2.

function relationships of the genome. Of particular importance is its application to nucleotide sequence determination that provides the primary information of the DNA molecule.

In the digestion of BKV DNA with *MboII*, we noticed an extra fragment, designated *MboII-Fx*, that migrated slightly slower than *MboII-F*. *MboII-Fx* and -F were present in about one-half molar amounts in most of the gel patterns obtained (Fig. 2 and 3; Tables 1 through 3). Incubation of isolated *MboII-Fx* with a large excess of *MboII* gave rise to *MboII-F* and *MboII-Q* (gel not shown). This has been confirmed by the results obtained from partial cleavage of several single-end labeled DNA fragments with *MboII* (Table 6). Since DNA fragments smaller than *MboII-Q* (about 50 base long), such as *MboII-V*, are generated readily, difficulty of cleavage due to the small size of DNA is unlikely. A similar observation was also reported by Yang et al. (37), that complete cleavage at the *AluI* and *HaeIII* sites at around map position 0.66 on the SV40 genome (where the DNA replication origin

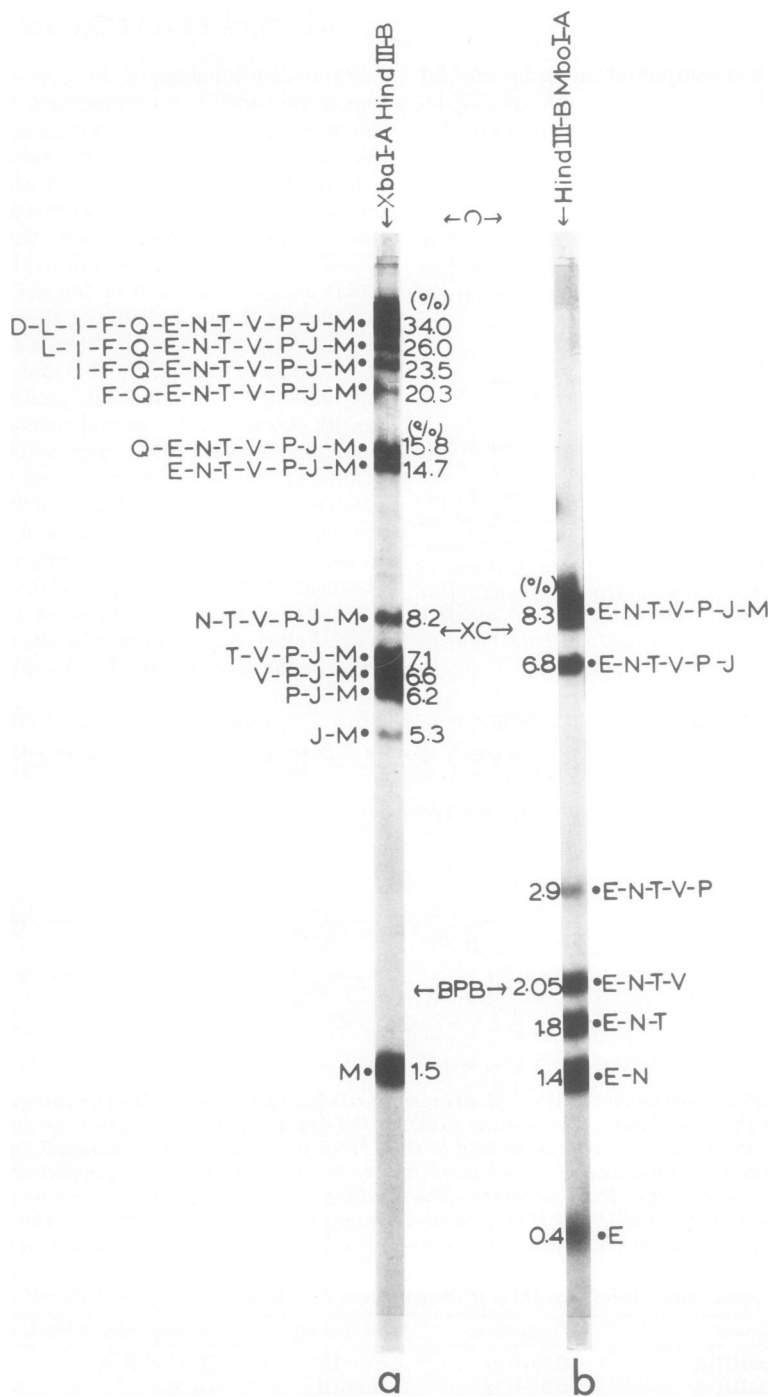


FIG. 8. Partial cleavage patterns of the single-end  $^{32}\text{P}$ -labeled DNA fragments with MboII. The single-end labeled restricted DNA fragments were cleaved with MboII under limited conditions as described in the text. Two typical sets of partial cleavage are shown: (a) using fragment XbaI-A HindIII-B (map positions 0.24 to 0.58) with the single labeled end at the HindIII site; and (b) using fragment HindIII-B MboI-A (map positions 0.51 to 0.58) with the single labeled end at the MboI site. The digests were fractionated electrophoretically in a 3.5% polyacrylamide gel. The partial MboII products that share the common  $^{32}\text{P}$ -labeled end were resolved and subjected to size estimation. The estimated sizes in percent genome length are indicated. The gel origin (0) is shown on top. The deduced order of the MboII fragments is indicated next to each band. The results obtained from (a) and (b) are complementary (see also Table 6).

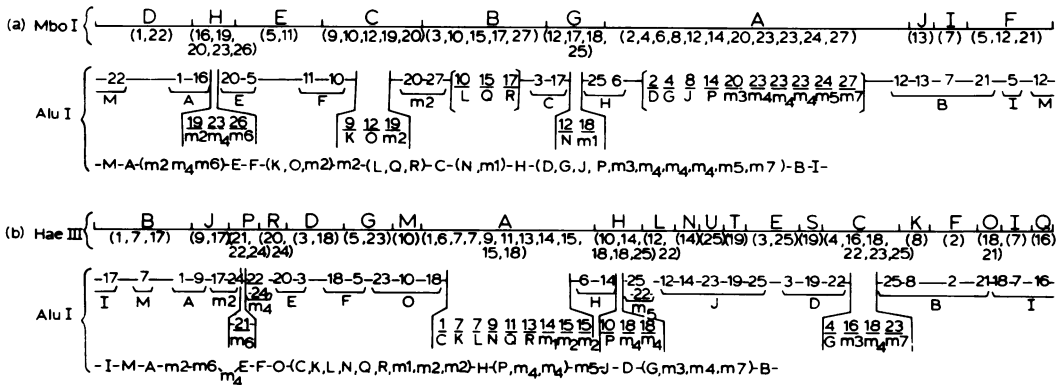


FIG. 9. Overlap analysis on (a) the MboI-AluI and (b) the HaeIII-AluI reciprocal cleavage patterns. The gel patterns of these two reciprocal cleavages are not shown. The procedures of overlap analysis are similar to those described in Fig. 7a.

TABLE 7. Single-end <sup>32</sup>P-labeled DNA fragments used for partial cleavage with AluI enzyme

DNA fragment	Map position	5'-Labeled site	Derived order of AluI fragments <sup>a</sup>
XbaI-A HindIII-A	0.72-0.97	HindIII	m3-m4-G-B-I—
XbaI-B HindIII-A	0.97-0.18	HindIII	E-m4-m6-m2-A-M <sub>1</sub>
XbaI-A HindIII-B	0.24-0.58	HindIII	P-m4-H-m1-N-C-Q-L-R—
XbaI-B HindIII-B	0.18-0.24	HindIII	F <sub>1</sub>
MboII-B HindIII-C <sup>b</sup>	0.60-0.72	HindIII	m7-D <sup>b</sup> -J
HhaI-A HindIII-C <sup>b</sup>	0.58-0.71	HindIII	m4-m5-J-D <sub>1</sub> <sup>b</sup>
HindIII-B XbaI-A	0.24-0.58	XbaI	F <sub>2</sub> -O-K-m2-m2-R-L-Q-C
HindIII-A XbaI-A	0.72-0.97	XbaI	M <sub>2</sub> -I-B-G—
HindIII-A XbaI-B	0.97-0.18	XbaI	M <sub>1</sub> -A-m2-m6-m4-E
HindIII-B XbaI-B	0.18-0.24	XbaI	F <sub>1</sub>

<sup>a</sup> The left-most fragment carries the <sup>32</sup>P-label.

<sup>b</sup> Three fragments of close sizes were observed as noted in Table 2.

maps) was difficult to achieve. Recently, it has been shown (32) that T-antigen protein binds specifically to the SV40 DNA at the aforementioned location. Thus, BKV DNA at the MboII site between MboII-F and -Q may be protected by a certain protein. Alternatively, an unusual DNA structure at this location may inhibit the cleavage of MboII.

In this study, we have located 3 cleavage sites of SacI, 22 sites of MboII, and 30 sites of AluI on the genome of BKV by means of reciprocal digestion as well as partial digestion. Since all the cleavage sites are positioned on the genome, a detailed multiple cleavage map (including those sites reported earlier) has been constructed, as shown in circle I of Fig. 1. This detailed map, derived from using 13 restriction enzymes, includes 90 cleavage sites. With the use of these enzymes, all of the restricted BKV(MM) DNA fragments are shorter than 350 nucleotides. These fragments are sufficiently short to allow complete sequence analysis by the chemical procedure (17). They are also suitable as primers in the enzymatic procedure of sequence analysis (24, 25).

#### ACKNOWLEDGMENTS

Technical assistance by J. Tomassini and S. Hanson during part of this study is gratefully acknowledged.

The work was supported by Public Health grants CA 14989, awarded by the National Cancer Institute, and by grant VC-216 from the American Cancer Society.

#### LITERATURE CITED

- Coleman, D. V., S. D. Gardner, and A. M. Field. 1973. Human polyoma virus infection in renal allograft recipients. *Br. Med. J.* 3:371-375.
- Dhar, R., C. J. Lai, and G. Khoury. 1978. Nucleotide sequence of the DNA replication origin for human papovavirus BKV: sequence and structural homology with SV40. *Cell* 13:345-358.
- Farrell, M. P., R. A. Mäntyjärvi, and J. S. Pagano. 1978. T antigen of BK papovavirus in infected and transformed cells. *J. Virol.* 25:871-877.
- Gardner, S. D. 1973. Prevalence in England of antibody to human polyomavirus (B.K.). *Br. Med. J.* 1:77-78.
- Gardner, S. D., A. M. Field, D. V. Coleman, and B. Hulme. 1971. New human papovavirus (B.K.) isolated from urine of renal transplantation. *Lancet* 1:1253-1257.
- Hirt, B. 1967. Selective extraction of polyoma DNA from infected mouse cell cultures. *J. Mol. Biol.* 26:365-369.
- Howley, P. M., G. Khoury, J. C. Byrne, K. K. Takemoto, and M. A. Martin. 1975. Physical map of the BK virus genome. *J. Virol.* 18:959-973.
- Howley, P. M., G. Khoury, K. K. Takemoto, and M.

- A. Martin.** 1976. Polynucleotide sequences common to the genomes of simian virus 40 and the human papovavirus JC and BK. *Virology* **73**:303-307.
9. **Howley, P. M., M. F. Mullarkey, K. K. Takemoto, and M. A. Martin.** 1975. Characterization of human papovavirus BK DNA. *J. Virol.* **15**:173-181.
  10. **Jung, M., U. Krech, P. C. Price, and M. N. Pyndiah.** 1975. Evidence of chronic persistent infections with polyomavirus (BK type) in renal transplant recipients. *Arch. Virol.* **47**:39-46.
  11. **Khoury, G., P. M. Howley, C. Garon, M. F. Mullarkey, K. K. Takemoto, and M. A. Martin.** 1975. Homology and relationship between the genomes of papovavirus, BK virus and simian virus 40. *Proc. Natl. Acad. Sci. U.S.A.* **72**:2563-2567.
  12. **Lecatsas, G., and O. W. Prozesky.** 1975. Excretion of morphological variants of human polyoma virus. *Arch. Virol.* **47**:393-397.
  13. **Lecatsas, G., O. W. Prozesky, J. Van Wyk, and H. E. Els.** 1973. Papovavirus in urine after renal transplantation. *Nature (London) New Biol.* **241**:343-344.
  14. **Major, E. O., and G. di Mayorca.** 1973. Malignant transformation of BHK<sub>21</sub> clone 13 cells by BK virus—a human papovavirus. *Proc. Natl. Acad. Sci. U.S.A.* **70**:3210-3212.
  15. **Mäntyjärvi, R. A., O. H. Heurman, L. Vihma, and B. Berglund.** 1973. A human papovavirus (BK), biological properties and seroepidemiology. *Ann. Clin. Res.* **5**:283-287.
  16. **Mason, D. H., Jr., and K. K. Takemoto.** 1976. Complementation between BK human papovavirus and a simian virus 40 tsA mutant. *J. Virol.* **17**:1060-1062.
  17. **Maxam, A. M., and W. Gilbert.** 1977. A new method for sequencing DNA. *Proc. Natl. Acad. Sci. U.S.A.* **74**:560-564.
  18. **Näse, L. M., M. Kärkkäinen, and R. A. Mäntyjärvi.** 1975. Transplantable hamster tumors induced with the BK virus. *Acta Pathol. Microbiol. Scand.* **83**:347-352.
  19. **Newell, N., C. J. Lai, G. Khoury, and T. J. Kelly, Jr.** 1978. Electron microscope study of the base sequence homology between simian virus 40 and human papovavirus BK. *J. Virol.* **25**:193-201.
  20. **Osborn, J. E., S. M. Robertson, B. L. Padgett, D. L. Walker, and B. Weisblum.** 1976. Comparison of JC and BK human papovaviruses with simian virus 40: DNA homology studies. *J. Virol.* **19**:675-684.
  21. **Portolani, M., G. Barbanti-Brodano, and M. LaPlaca.** 1975. Malignant transformation of hamster kidney cells by BK virus. *J. Virol.* **15**:420-422.
  22. **Reese, J. M., M. Reissig, R. W. Daniel, and K. V. Shah.** 1975. Occurrence of BK virus and BK virus-specific antibodies in the urine of patients receiving chemotherapy for malignancy. *Infect. Immun.* **11**:1375-1381.
  23. **Rundell, K., P. Tegtmeyer, P. J. Wright, and G. di Mayorca.** 1977. Identification of the human papovavirus T antigen and comparison with the simian virus 40 protein A. *Virology* **82**:206-213.
  24. **Sanger, F., and A. R. Coulson.** 1976. A rapid method for determining sequences by primed synthesis with DNA polymerase. *J. Mol. Biol.* **94**:441-448.
  25. **Sanger, F., S. Nicklen, and A. R. Coulson.** 1977. DNA sequencing with chain-terminating inhibitors. *Proc. Natl. Acad. Sci. U.S.A.* **74**:5463-5467.
  26. **Shah, K. V., R. W. Daniel, and J. Strandberg.** 1975. Sarcoma in a hamster inoculated with BK virus, a human papovavirus. *J. Natl. Cancer Inst.* **54**:945-949.
  27. **Shah, K. V., R. W. Daniel, and R. M. Warszawski.** 1973. High prevalence of antibodies to BK virus, an SV40-related papovavirus, in residents of Maryland. *J. Infect. Dis.* **128**:784-787.
  28. **Shah, K. V., H. L. Ozer, H. N. Ghazey, and T. J. Kelly, Jr.** 1977. Common structural antigen of papovaviruses of the simian virus 40-polyoma subgroup. *J. Virol.* **21**:179-186.
  29. **Takemoto, K. K., and M. A. Martin.** 1976. Transformation of hamster kidney cells by BK papovavirus DNA. *J. Virol.* **17**:247-253.
  30. **Takemoto, K. K., and M. F. Mullarkey.** 1973. Human papovavirus BK strain: biological studies including antigenic relationship to simian virus 40. *J. Virol.* **12**:625-631.
  31. **Takemoto, K. K., A. S. Rabson, M. F. Mullarkey, R. M. Blaese, C. F. Garon, and D. Nelson.** 1974. Isolation of papovavirus from brain tumor and urine of a patient with Wiskott-Aldrich syndrome. *J. Natl. Cancer Inst.* **53**:1205-1207.
  32. **Tjian, R.** 1978. The binding site on SV40 DNA for a T antigen-related protein. *Cell* **13**:165-178.
  33. **Van der Noordaa, J.** 1976. Infectivity, oncogenicity and transforming ability of BK virus and BK virus DNA. *J. Gen. Virol.* **30**:371-373.
  34. **Wright, P. J., G. Bernhardt, E. O. Major, and G. di Mayorca.** 1976. Comparison of the serology, transforming ability, and polypeptide composition of human papovaviruses isolated from urine. *J. Virol.* **17**:762-775.
  35. **Wu, R., E. Jay, and R. Roychoudhury.** 1976. Nucleotide sequence analysis of DNA. *Methods Cancer Res.* **12**:87-176.
  36. **Yang, R. C. A., A. Van de Voorde, and W. Fiers.** 1976. Cleavage map of the simian virus 40 genome by the restriction endonuclease III of *Haemophilus aegyptius*. *Eur. J. Biochem.* **61**:101-117.
  37. **Yang, R. C. A., A. Van de Voorde, and W. Fiers.** 1976. Specific cleavage and physical mapping of simian virus 40 DNA by the restriction endonuclease of *Arthrobacter luteus*. *Eur. J. Biochem.* **61**:119-138.
  38. **Yang, R. C. A., and R. Wu.** 1978. BK virus DNA: cleavage map and sequence analysis. *Proc. Natl. Acad. Sci. U.S.A.* **75**:2150-2154.
  39. **Yang, R. C. A., and R. Wu.** 1978. Cleavage map of BK virus DNA with restriction endonuclease *MboI* and *HaeIII*. *J. Virol.* **27**:700-712.